

OBSERVATION AND IMPLICATION OF MHD MODES FOR THE HYBRID SCENARIO IN JET

P. Belo ¹, P. Buratti ², R. J. Buttery ³, T. C. Hender ³, D. F. Howell ³, A. Isayama ⁴, E. Joffrin ⁵,
M. F. F. Nave ¹, G. Sips ⁶ and JET-EFDA contributors ^b

¹Associação EURATOM/IST, Centro de Fusão Nuclear, 1049-001 Lisbon, Portugal

²EURATOM/ENEA Fusion Association, via E. Fermi 45, 00044, Frascati, Italy

³Euratom/UKAEA Fusion Association, Culham Science Centre, Abingdon, OX143DB

⁴Japan Atomic Energy Research Institute, Naka-gun, Ibaraki-ken, 311-0193 Japan.

⁵Association EURATOM-CEA, CEA Cadarache, F13108, St. Paul lez Durance, France

⁶Max-Planck-Institut für Plasmaphysik, IPP-EURATOM Assoziation, Boltzmannstrasse 2, D-85748, Garching, Germany

Introduction

The hybrid scenarios (HS) of advanced tokamak operation are characterised by the presence of a wide central region with magnetic shear very close to zero and central q-values between 1 and 1.5 [1]. The main advantages of this mode of operation are improved energy confinement and improved MHD stability leading to a higher β_N limit. This paper deals with MHD modes observed in JET HS discharges where the target q-profile is obtained by a combination of LHCD, NBI and ICRH heating. MHD modes such as (3,2), (4,3), (5,3) NTMs, fishbone instabilities, sawtooth and ELMs were observed.

In this paper the focus will be on the triggering types of the (3,2) NTM. The β_N versus ρ^* will be determined at the (3,2) NTM onset. The effect of the (3,2) NTM on the energy confinement will be examined, as well as the influence of different MHD mode types on the (3,2) NTM island width and the influence of the (3,2) NTM on the central electron and ion temperatures.

Triggering Processes

In the JET database for the HS three types of triggering for the (3,2) NTM (figure 1) were observed: (1) as a (3,2) tearing mode that started during the L-mode phase; (2) during H-mode and in the presence of (1,1) modes; (3) spontaneously during H-mode. During the L mode the collisionality regime is in the Pfirsch-Schlüter. In this regime the bootstrap current is small and so the (3,2) mode can only be current driven and it is therefore probably triggered when the stability parameter Δ' is positive. The (3,2) mode becomes a NTM after

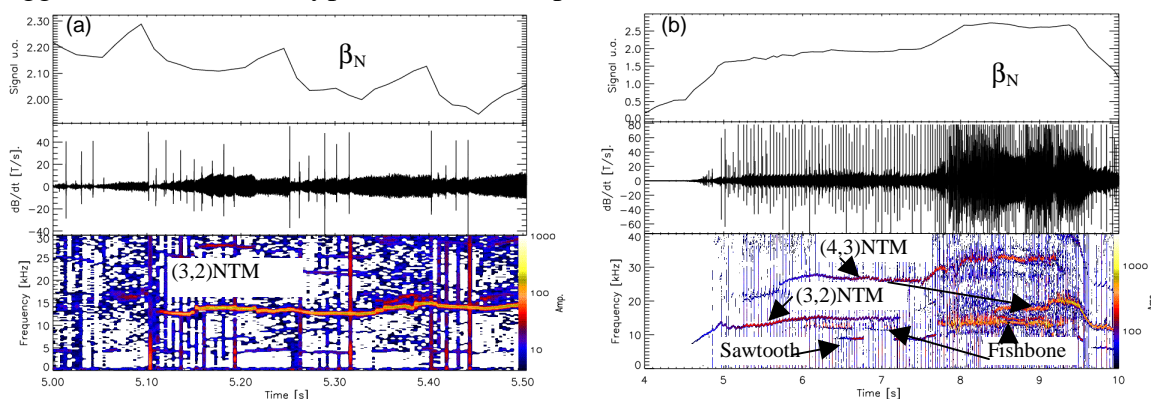


Figure 1. Spectrograms of magnetic signal for the pulses no: 60927 and 57822. In (a) the triggering is type (3) with $\beta_N = 2.18$. In (b) the (3,2) NTM starts as a tearing mode at 4.19 s with β_N and disappears at 4.73 s, this is type (1). The time of triggering of the (3,2) NTM onset is at 4.8 s.

^b appendix of J. Pamela, JET-EFDA Team in Fusion Energy 2002 (Proc. 20th Int. Conf., Lyon, 2002), IAEA Vienna 2001 CD-Rom file PD/1

energy 2002 (Proc. 20th Int. Conf., Lyon, 2002), IAEA

the L to H mode transition when the bootstrap current is significant. NTMs the (3,2) island growth rate was exponential, similar to those plasmas where the onset coincides with the first sawtooth crash after the L to H transition.

For the spontaneous observed in low β_N H transition.

β_N and ρ^*

Historically the assumption has been that the (3,2) NTM would be triggered when the plasma reached a certain value of β_N/ρ^* [3], in the conventional ELMy H-mode plasmas with magnetic shear >0 . In figure 2 is plotted the values of ρ^* versus β_N at the (3,2) NTM onset for the pulses of $s > 0$ database [2] and HS database. The pulses without the (3,2) NTM for the HS database are also included. This figure shows that the HS pulses with $T_e \approx T_i$ and pulses with $s > 0$ have similar values of β_N when the NTM is triggered. Like in previous studies the relation between β_N and ρ^* is a necessary but not sufficient condition for the triggering [2, 4]. In the HS scenario the (3,2) NTM onset is more probable for $\beta_N > 1.4$, while the lowest β_N correspond to the (3,2) tearing mode. Thus we see that the (3,2) NTM onset occurs throughout the operational space of β_N versus ρ^* for discharges. This indicates that other factors must be playing a role; making understanding the seeding process crucial.

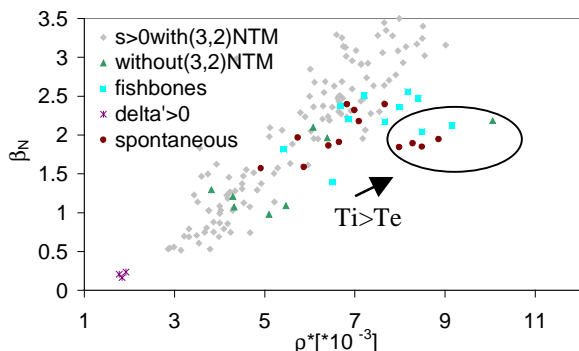


Figure 2: β_N versus ρ^* at the (3,2) NTM onset for HS pulses data base and without at the maximum value of β_N and pulses with (3,2) NTM for $s > 0$ pulses

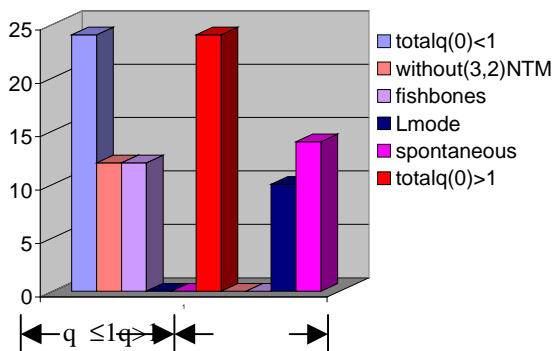


Figure 3: Number of JET pulses in the hybrid scenario database for different types of (3,2) triggering

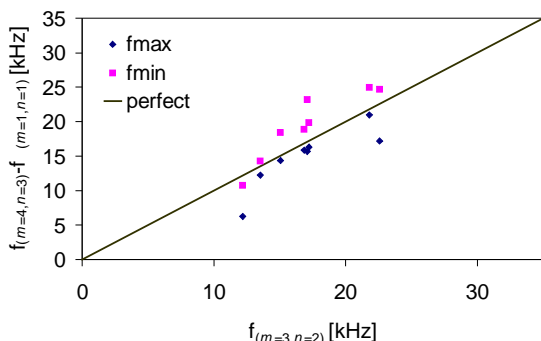


Figure 4: The difference between the frequency of the (4,3) mode and the minimum (pink) and maximum (blue) frequencies of the fishbone instabilities versus the frequency of the (3,2) NTM

Thus we see that the (3,2) NTM onset occurs throughout the operational space of β_N versus ρ^* for discharges. This indicates that other factors must be playing a role; making understanding the seeding process crucial.

Seeding

The total number of pulses in the HS database was 48. In half of them neither the fishbone nor the sawtooth were observed and for these pulses $q(0) > 1$ was assumed. In all these pulses a (3,2) NTM was triggered (figure 2). In the pulses, in which the (3,2) NTM was triggered spontaneously the shear is small at $q = 1.5$. In the other half of the pulses from the HS database (figure 3), the $q(0) \leq 1$ was assumed when, at least the fishbone instabilities were observed. In 12 of these pulses the (3,2) NTM was not observed but the sawtooth and the fishbone instabilities were present. In only a few pulses with a (3,2) NTM were sawteeth present and in these cases their period was very long, (minimum of 0.3 s) with most of the NTMs onsets occurring between two crashes. This is a clear indication that the (1,1) mode of the fishbone instabilities were the best

candidates for the three wave mode non-linear coupling as was found for plasmas [2, 5]. In figure 4 is plotted the difference of the maximum frequency of the (1, 1) fishbone and the (4,3) NTM closest to the time of onset, against the (3,2) NTM frequency. In this plot is also included the perfect frequency match for the non-linear three wave mode coupling and this is between the maximum and the minimum fishbone frequency for all the pulses except one. This indicates three wave coupling as a possible mechanism for triggering these HSNTMs.

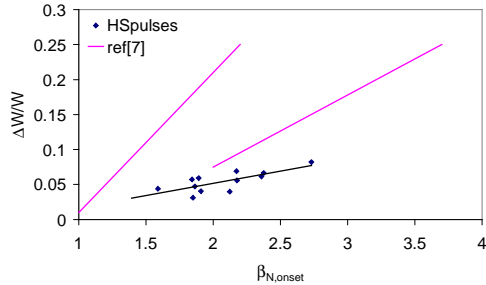


Figure 5: Relative confinement reduction (difference in plasma energy content at mode onset and after its saturation, normalised to the energy at NTM onset) due to (3,2) NTMs versus β_N at NTM onset for jet. The trend line in pink is for >0 pulses from ref.[7].

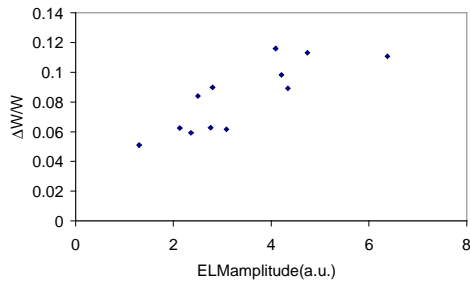


Figure 6: Relative confinement reduction (difference in plasma energy before and after the ELM, normalised to the energy before the ELM) due to single ELM

Energy Confinement

In positive shear plasmas a reduction typically of 10%-20% in energy content is observed after the (3,2) NTM onset (e.g. [6]). In figure 5 it is clearly seen that the decrease in energy confinement is much lower for HS pulses and also that the increase of confinement degradation with β_N is also lower. A possible explanation is the island width that is in average around 2 to 6 cm while in $s>0$ plasmas are of the order of 10 cm. A possible explanation is also that the $q=1.5$ will be at smaller minor radius, and so the pressure drop from the mode will be over a smaller volume of plasma.

It was not possible, in all the pulses in the HS database, to determine the energy loss due to the (3,2) NTM because, as it can be seen in figure 6, the energy loss due to an ELM can be higher than for the (3,2) NTM for the highest ELM amplitude.

Island width

The island width is proportional to the square root of the magnetic perturbation for a constant shear and radius of the resonance surface. Figure 7 shows that the island width decreases during ELMs. This was more evident for pulses with $q(0) > 1$. The island width is not only perturbed by the ELMs but also by the (4,3) NTM unlike in ref [8] the (1,1) mode is not present. This is clearly seen in figure 8, the amplitude of the (3,2) NTM decreases when the (4,3) NTM increased and vice versa. The amplitude of the (4,3) NTM at the wall was very small and to compare with the (3,2) NTM amplitude was

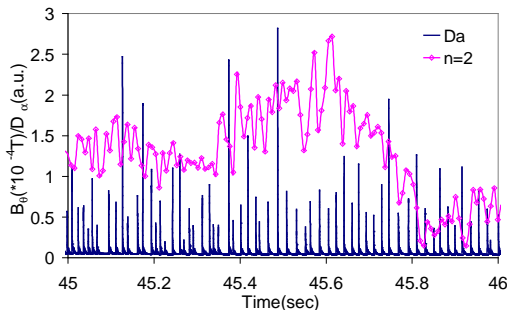


Figure 7: Radial perturbation of the magnetic field ($W \propto \tilde{B}_r^2$) for (3,2) NTM and the D_α signal for the pulse no: 60926

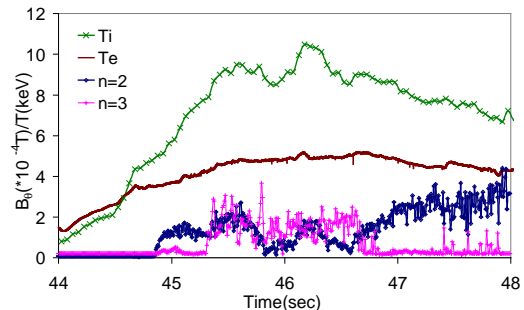


Figure 8: Mode amplitude for the (3,2) NTM (blue), 5* the amplitude of the (4,3) NTM for comparison (pink); electron temperature at $R=3.2$ (brown); ion temperature at $R=3.14$ (green) for the pulse no: 60926

necessary to multiply it 5 times. Figure 8 also shows that after the disappearance of (4,3) NTM, the (3,2) NTM grows to a saturated width and the core ion temperature decreases more than the core electron temperature.

CONCLUSIONS

In all the pulses with $q(0) > 1$ (3,2) NTM onset occurred, possibly due to the low shear at the $q = 1.5$ resonance surface.

For the same ρ^* value the HS pulses with $T_e \approx T_i$ and pulses with $s > 0$ have similar values of β_N at the (3,2) NTM onset and this was more probable to occur for $\beta_N > 1.4$. For pulses with $T_i > T_e$ the usual β_N, r^* scaling was not followed.

In HS scenarios (3,2) NTMs have a much smaller effect on the confinement than standard ELMy H-modes. In these scenarios ELMS can reduce the energy content more than the (3,2) NTM

The (3,2) island width was affected by other MHD modes like ELMs and the (4,3) NTM (even though there is no (1,1) mode present).

The (3,2) NTM affects the ion central temperature more than the electron temperature. The observations of larger MHD effects on T_i rather than on T_e and confinement are similar to observations from JET hot ion H-modes [9].

ACKNOWLEDGMENT

This work, which has been supported by the European Communities and the Instituto Superior Técnico (IST) under the Contract of Association between the European Atomic Energy Community and IST, was performed under the European Fusion Development Agreement. The views and opinions expressed here do not necessarily reflect those of the European Commission and IST.

REFERENCE:

- [1] SIPS, G., 30th EPS, St. Petersburg, Russia 7-11 July 2003
- [2] BELO, P. *et al*, To be submitted to Plasma Physics and Controlled Fusion
- [3] BUTTERY, R.J., *et al*, Plasma Phys. and Control. Fusion, **42**(2000)B61
- [4] BUTTERY, R.J., *et al*, Nuclear Fusion, **44**(2004)678
- [5] NAVE, M.F.F. *et al*, Nuclear Fusion **43**(2003)179
- [6] HENDER, T.C., *et al*, this EPS poster.
- [7] GÜNTHER, S., *et al*, Nuclear Fusion, **44**(2004)524
- [8] PINCHES, S., *et al*, 30th Conference of Plasma Physics and Controlled Fusion, San Petersburg, 2003
- [9] NAVE, M.F.F. *et al*, Nuclear Fusion **35**(1995)409